

Surface Modification via Chain End Segregation in Polymer Blends

T. F. Schaub, G. J. Kellogg, and A. M. Mayes*

Department of Materials Science and Engineering, Massachusetts Institute of Technology, Cambridge, Massachusetts 02139

R. Kulasekere, J. F. Ankner, and H. Kaiser

Research Reactor Center, University of Missouri-Columbia, Columbia, Missouri 65211

Received July 25, 1995; Revised Manuscript Received January 2, 1996[®]

ABSTRACT: We have explored the use of chain end segregation as a means of controlling the properties of a polymer surface. Thin film blends of homopolystyrene (PS) and PS synthesized with low-energy oligotetrafluoroethylene chain ends (PS-TFE) were studied using neutron reflectivity. The fraction of PS-TFE that localizes near the surface was found to increase as a function of its concentration in the blend. Contact angle measurements indicate corresponding reductions in the surface tension due to the surface localization of the TFE chain ends. For a 10% blend of 6000 mol wt PS-TFE in 3×10^5 mol wt PS, the surface coverage of fluorocarbon ends was found to be >20%. A free energy model of the blends gives good qualitative agreement with the experimental results.

Introduction

In many applications, the properties desired at a polymer surface, such as adhesion, wettability, gas impermeability, stain resistance, or biocompatibility, are often specific and distinct from the bulk properties of the material. Conventionally, control of surface properties is achieved by surface modification through various chemical or physical processes, such as plasma or flame treatment, chemical reaction, surface grafting, or metal coating.^{1,2} Many of these kinetically governed reaction mechanisms allow relatively little control over the equilibrium surface composition and structure. Additionally, such processes may be expensive and difficult to model. Other techniques for controlling surface properties include the incorporation of small molecules or oligomeric additives which migrate to the polymer surface. Such additives may compromise the polymer's bulk physical properties, however, and, because they are not strongly bound to the polymeric matrix, may be removed by evaporation, dissolution, or wear.

An alternative method of polymer surface modification may be through the preferential segregation of functionalized chain ends. Recent investigations by several groups have examined the effects of end-functionalization on the surface composition and properties of different model systems. Neutron reflectometry and X-ray photoelectron spectroscopy (XPS) measurements on fluorocarbon-terminated polystyrenes have demonstrated a surface excess of the low-energy fluorocarbon tails with a subsequent reduction in surface tension.^{3–7} By contrast, a surface depletion of high-energy chain ends has been observed for polystyrenes synthesized with carboxylic acid end groups⁵ and for amine-terminated poly(dimethylsiloxane).^{8,9}

At polymer–polymer interfaces, the technological use of chain end segregation for modifying interfacial properties has already been demonstrated. Koberstein and co-workers used the association of acid- and base-functional end groups to reduce the interfacial tension between immiscible polybutadiene and poly(dimethylsiloxane).¹⁰ Norton et al.¹¹ achieved 1 order of magnitude improvement in interfacial fracture toughness

between polystyrene and epoxy through segregation of carboxylic acid chain ends which grafted to the epoxy surface. Interfacial grafting of functionalized chain ends is also the basis of some reactive blending schemes designed to compatibilize and strengthen immiscible polymer blends during melt processing.^{12,13}

While technologically promising, surface control via chain end segregation may be prohibitively expensive due to the relatively high cost of synthesizing end-functionalized polymers. An alternative is to blend small amounts of end-functionalized polymers with low-cost, widely available commodity plastics (A-B/A blends). The anchoring portion of the end-functionalized polymer is chosen to match the matrix plastic, while the end-functionalized tail is selected to deliver the desired surface properties. Previous studies on analogous blends of A-B diblock copolymers and A homopolymers have shown that large surface coverages of a lower surface energy B block can be achieved with relatively small bulk concentrations of the diblock.¹⁴ By employing end-modified polymers instead of block copolymers as surface modification agents, one might avoid the formation of micelles which can adversely affect the physical properties of the bulk, such as optical transparency.

The fraction of end-modified material which segregates to the surface in A-B/A blends will depend on several system parameters. Primarily, the effective reduction in surface tension due to the surface localization of low-energy tails is expected to drive the segregation of the end-modified components. However, the relative molecular weights of the two components should also play a role, as conformational entropy considerations favor a surface excess of the lower molecular weight component.¹⁵ The surface coverage of chain ends will be limited, however, by unfavorable stretching of the anchored chains beyond their random flight conformation when the packing density of chain ends at the surface increases. Finally, the entropy of mixing of the blend components favors their complete mixing and is thus expected to counterbalance the reduction in surface tension, particularly for very thin films where surface segregation can result in a significant depletion of the fraction of end-modified chains in the remainder of the

[®] Abstract published in *Advance ACS Abstracts*, May 1, 1996.

Table 1. Molecular Weight Characteristics of Polymers

composition	M_n	M_w/M_n
PS	392 000	1.02
dPS	7 540	1.57
dPS	269 000	1.12
PS-TFE	6 310	1.16
dPS-TFE	7 230	1.26

system. The balance of these forces dictates the degree of surface coverage of end-modified chains.

This work explores the use of end-modified polymers with low-energy tails as surface modification agents in A-B/A blends. Such systems are of potential interest for commercial applications requiring nonstick, anti-stain, or water-repellent surfaces. In particular, surface segregation in thin films of high molecular weight polystyrene blended with low molecular weight fluorocarbon-end-modified polystyrene (denoted here as PS-TFE) is examined as a function of the blend composition. Similar work on blends containing 15 wt % PS-TFE with polystyrene of comparable molecular weight was reported previously by Richards and co-workers.⁶ In their study, static secondary ion mass spectroscopy was used to determine the fraction of end-modified material at the surface by perdeuterating either component and comparing the signal intensities from $C_7H_7^+$ and $C_7D_7^+$ ions. Herein, neutron reflectivity is performed with deuteration of either the homopolymer or end-functionalized polymer to enhance the scattering contrast between the blend components. The data are fit using model profiles which allow us to determine quantitatively the degree of surface segregation of PS-TFE, as well as the composition profile across the film. Contact angle measurements are then performed to examine the corresponding reduction in surface tension due to the surface localization of the fluorocarbon chain ends. Finally, a model for surface segregation in A-B/A blends is developed to compare with experimental results and make further predictions regarding the dependence of segregation on concentration, molecular weight of the components, and sample thickness.

Experimental Section

Perdeuterated homopolystyrenes (dPS) and low molecular weight PS-TFE and dPS-TFE were synthesized using inert gas anionic methods. The dPS homopolymers were initiated with *sec*-butyllithium and terminated with excess methanol. End-modified polystyrenes were initiated using *sec*-butyllithium and terminated with excess (tridecafluoro-1,1,2,2-tetrahydrooctyl)-1-dimethylchlorosilane.³ After purification, the degree of functional termination was determined by NMR to be in excess of 90%. A more complete discussion of the synthesis and characterization of the functionally terminated polystyrenes is provided elsewhere.^{3,7} Homopolystyrene with a molecular weight of 400K was purchased from Aldrich Chemicals. Molecular weight characteristics of the polymers used in this study are listed in Table 1.

Blends of varying concentration were prepared by codissolving 7K dPS-TFE and 400K PS or 6K PS-TFE and 300K dPS in toluene. A series of control blends of 7K dPS in 400K PS were additionally prepared to isolate the role of molecular weight from that of the fluorocarbon ends in the observed segregation. The polymer solutions were filtered using Milipore GVHP013 0.22 μ m filters to remove dust.

Polished silicon wafers—for NR, 10 cm in diameter (Semiconductor Processing); for contact angle measurements, ca. 1 cm² wafer sections (Exsil)—were immersed for a 24 h period in chromic-sulfuric acid solution (Fisher Chemicals) to remove any hydrocarbon impurities. The wafers were subsequently rinsed with deionized water (18.2 M Ω cm). Thin films were prepared by spin coating the filtered solutions onto the Si

Table 2. Material Constants Used in Reflectivity Analysis

material	density (g/cm ³)	$b/V (\times 10^{-6} \text{ \AA}^{-2})$
<i>sec</i> -butyl	0.77	-0.01
TFE	1.05	2.27
PS	1.04	1.43
dPS	1.08	6.10
Si	2.32	2.08
SiO ₂	2.20	3.05

wafers. Film thicknesses were measured prior to annealing using a Gaertner Scientific Corp. L3W26C.488.830 ellipsometer. Samples were annealed in an evacuated oven at 140 °C for 6–8 h to achieve equilibrium.

Neutron reflectivity (NR) measurements were performed on the grazing angle neutron spectrometer (GANS) at Missouri University's Research Reactor Facility (MURR) in Columbia, Missouri.¹⁶ A monochromatic neutron beam of wavelength 2.35 Å was used to obtain reflectivity data in a q range of 0–0.14 Å⁻¹. After reduction and normalization, reflectivity profiles were fitted following procedures outlined in earlier publications.^{17,18} Model scattering length density (b/V) profiles were generated by subdividing the air and substrate interfaces into many incremental layers of ca. 5 Å in thickness. The b/V of each layer was calculated by modeling the concentration profile at each interface as a Gaussian distribution. (In practice, NR is known to be somewhat insensitive to the functional form chosen for modeling graded interfaces.) Theoretical reflectivities were then calculated from the model b/V profiles using the Parratt formalism¹⁹ and compared to the experimental data. Model parameters including the total film thickness, the half-width of the interfacial region, and the fraction of material segregated to each interface were varied iteratively while maintaining conservation of the two blend components in the film to achieve a best fit to the data by minimizing the error between the calculated and experimental reflectivities. Calculated scattering length density values for the materials used in this study are listed in Table 2.

Contact angle measurements were taken on a VCA2000 video contact angle system (ASE, Inc.) with the assistance of Prof. M. F. Rubner at MIT. This method of measuring surface tension is based on the Young equation for contact-angle equilibrium. For a liquid drop on an ideal substrate, the relation between the contact angle and the various interfacial tension components is given by¹

$$\cos \theta_e = \frac{\gamma_{SV} - \gamma_{SL}}{\gamma_{LV}} \quad (1)$$

where L, V, and S stand for liquid, vapor, and solid, respectively, and θ_e is the equilibrium contact angle. In these experiments, sample surfaces were advanced upward toward a droplet of water resting on the tip of a syringe. Upon contact, the water droplet instantly wet the sample surface. The image of the sessile drop was immediately captured on video, from which contact angle values were determined. While surface reconstruction is not expected to play a role in the time frame of the measurements described here, other studies suggest these surfaces do reconstruct on extended contact with water.⁴

Results and Discussion

Reflectivity Studies. Figure 1 displays the NR profiles for the 7K dPS/400K PS blend studies. Profiles for the blends composed of 2%, 5%, 10%, and 20% dPS are shown, each offset by a factor of 10 for display purposes. The high-frequency oscillations present in each of the profiles are characteristic of the film thickness and result from the interference between reflections from the surface/film and substrate/film interfaces. A notable trend present in the data is the damping of the thickness oscillations as the dPS concentration increases. This is due primarily to the decrease in contrast between the film and the Si wafer. For a 15%

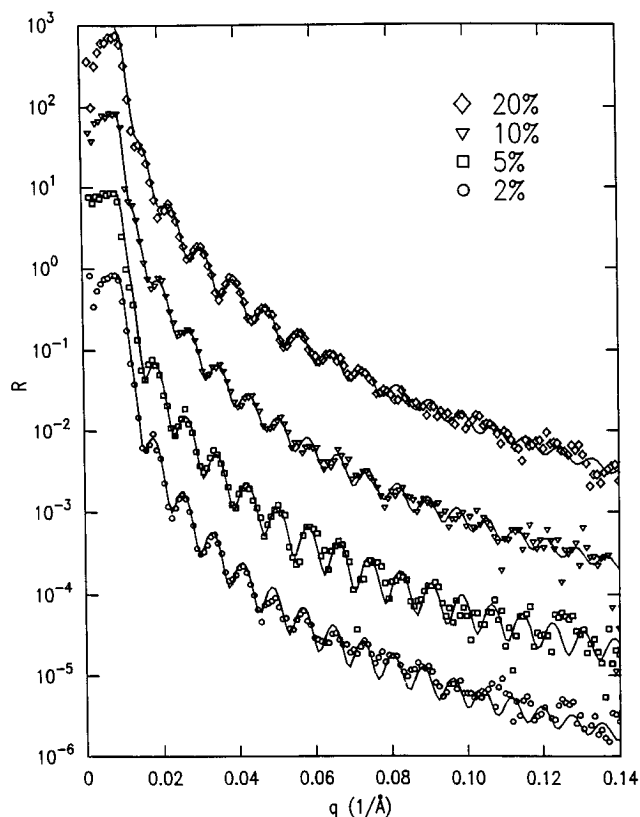


Figure 1. Fitted reflectivity data for the 7K dPS/400K PS control blends composed of 2%, 5%, 10%, and 20% dPS. Profiles are offset by factors of 10.

dPS/85% PS blend, the scattering length density (b/V) is approximately equal to that of Si; hence one would not expect a strong interference for this concentration range.

Figure 2 displays the NR profiles for 7K dPS-TFE/400K PS blends composed of 2%, 5%, 10%, and 20% dPS-TFE, again offset by factors of 10. In these systems the thickness oscillations are damped even more sharply with increasing concentration of dPS-TFE. What is more important to note, however, is that, compared with the profiles from the control samples, the dPS-TFE systems show greater measured reflectivities at high q . This is clearly indicated by comparing the 20% concentrations for each system at $q = 0.14 \text{ \AA}^{-1}$. The dPS-TFE blend shows a significantly larger measured reflectivity, which is strongly indicative of excess dPS-TFE at the film surface. This can be understood qualitatively by considering the samples as effective 2-layer systems with the upper layer being the (high b/V) near-surface region of the film and the lower layer being the remainder of the film and substrate, which have comparable b/V values for this concentration range. A sharp vacuum/upper layer interface is assumed, while the interface between the upper and lower layers is diffuse. For such a system, the thickness-averaged reflectivity is approximated for large values of q as:¹⁷

$$\langle R(q) \rangle = (4\pi^2/q^4) \{ (b/V)_1^2 + [(b/V)_2 - (b/V)_1]^2 \exp(-q^2 \sigma^2) \} \quad (2)$$

where σ is the half-width of the interface between the layers. With increasing q , $\langle R(q) \rangle$ tends to the value $(4\pi^2/q^4)(b/V)_1^2$. Hence for larger degrees of surface segregation of the deuterated component, the reflectivity at high angles will be larger.

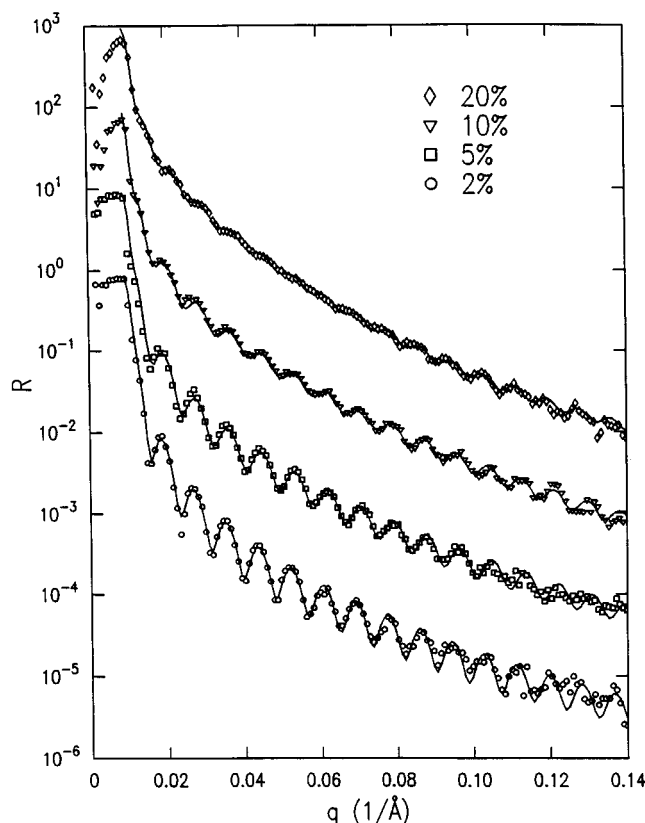


Figure 2. Fitted reflectivity data for the 7K dPS-TFE/400K PS A-B/A blends composed of 2%, 5%, 10%, and 20% dPS-TFE.

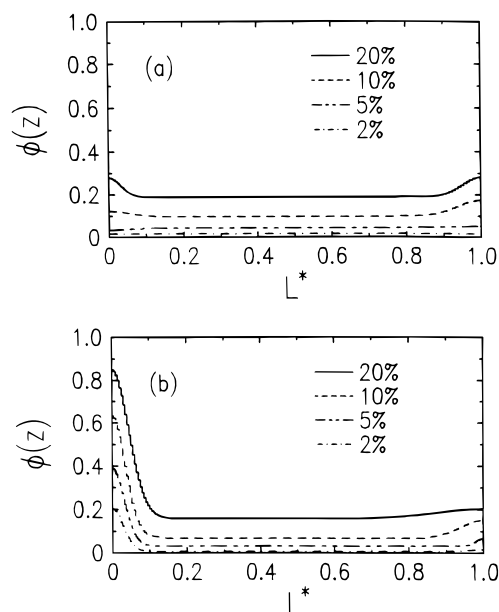


Figure 3. Volume fraction profiles of the 7K dPS (a) and 7K dPS-TFE (b) blend components as a function of normalized sample thickness, derived from the fits in Figures 1 and 2.

A more quantitative picture of the surface segregation in these systems was obtained by fitting the NR data, as shown in Figures 1 and 2. Volume fraction profiles derived from these fits are illustrated in Figure 3, where $\phi(z)$, the local volume fraction of 7K dPS or 7K dPS-TFE, is plotted as a function of the normalized sample depth, L^* , which is defined as:

$$L^* = \frac{z}{L} \quad (3)$$

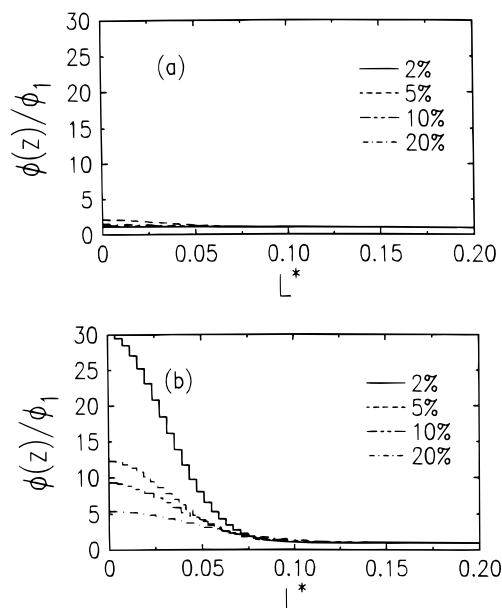


Figure 4. Surface excess profiles for the 7K dPS (a) and 7K dPS-TFE (b) blend components as a function of the normalized sample thicknesses.

where z is the absolute depth perpendicular to the sample surface and L is the total film thickness ($\langle L \rangle$ is 736 and 772 Å for dPS-TFE/PS blends and dPS/PS blends, respectively). In both cases an enhanced concentration of low molecular weight material can be observed in the region near the surface, i.e., near $L^* = 0$. In the control samples, a slight excess of the 7K dPS material to the surface is observed, which may be explained by several factors. First, theoretical arguments suggest that the low molecular weight component in a bimodal blend will tend to locate preferentially to the surface in order to minimize loss of conformational entropy at the material boundary. Self-consistent field calculations by Kumar and co-workers¹⁵ have shown that surface enhancement due to conformational effects alone is typically on the order of several percent over the bulk concentration for blends with large molecular weight disparities. Indeed, the surface tension of polystyrene is empirically known to have a significant molecular weight dependence, as noted in the Appendix (eq A.4). In our system, the ratio of the component molecular weights is large (ca. 50), so such effects should be detectable at higher concentrations of the 7K material.

Isotopic effects may also play a role in the segregation of the 7K dPS to the surface. The difference in polarizability between deuterated and normal polystyrene gives a slightly lower surface energy for dPS, which could give rise to the observed excess. Such effects can be very pronounced for high molecular weight isotopic blends close to the UCST.^{20–22} Finally, the presence of the butyl group initiator fragment at one chain end may have a role in the observed segregation. Surface adsorption of the low-energy initiator fragment has been observed for pure PS-TFE materials.^{5,7}

For blends containing the end-functionalized material, a much larger segregation is observed at the surface due to the low-energy fluorocarbon chain ends. The fraction of dPS-TFE at the surface increases significantly with bulk concentration. The degree of excess of dPS or dPS-TFE at the surface can also be shown as a function of depth, as seen in Figure 4, where the local concentration, $\phi(z)$, is normalized by the experimentally

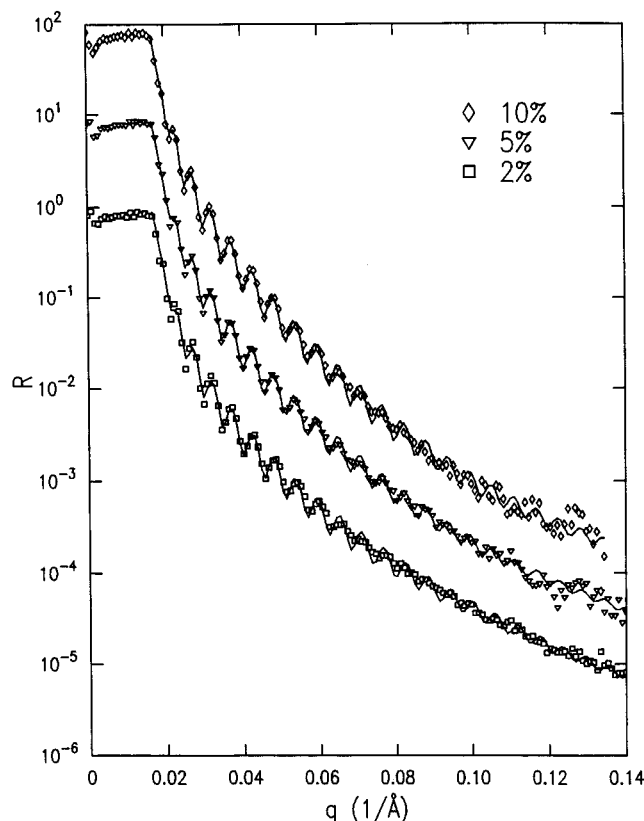


Figure 5. Fitted reflectivity data for the 6K PS-TFE/300K dPS blends composed of 2%, 5%, and 10% PS-TFE.

determined concentration in the film's interior, ϕ_1 . For the 7K dPS blends there is very little enhancement of the low molecular weight additive at the surface for all concentrations. In sharp contrast, the 7K dPS-TFE blends show remarkable surface excesses over bulk levels. The degree of excess decreases monotonically with increasing bulk concentration of dPS-TFE (ϕ_B), with the 2% blend demonstrating a surface excess of 30 times and the 20% blend showing a surface excess of 5 times.

The next set of reflectivity experiments was performed to address the effects of isotopic labeling in this investigation. Reflectivity profiles for blends composed of 2%, 5%, and 10% 6K PS-TFE in 300K dPS are shown in Figure 5. The reflectivity profiles are notably different in nature from the previous experiments in two regards. First, critical angles have nearly doubled to $q = 0.02 \text{ \AA}^{-1}$ for these profiles, compared to the dPS-TFE/PS blends in Figure 2, due to the higher scattering length density of the dPS matrix. Second, the reflectivity at high q values decreases with increasing concentration of end-modified material, compared to Figure 2 which shows the opposite trend. Indeed, comparing the measured reflectivities for the two 10% blends at $q = 0.14 \text{ \AA}^{-1}$ shows nearly 1 order of magnitude lower value for the PS-TFE/dPS system, although the average b/V of the film is significantly higher. This data visually suggests that it is the low-scattering length density material which localizes at the surface in these blends.

Volume fraction profiles calculated from the scattering length density profiles for the 6K PS-TFE/300K dPS blends are presented in Figure 6. The nature of the profiles is identical with those in Figure 3, with a large surface enhancement of PS-TFE. No selective segregation of dPS to the surface was observed, indicating that any isotopic effects are dominated by the

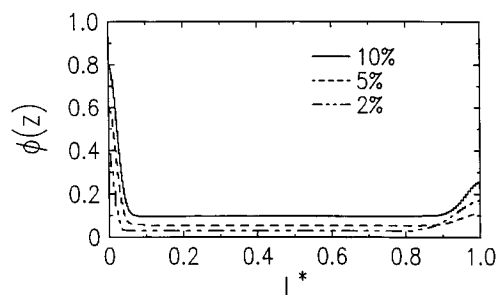


Figure 6. Volume fraction profiles for the 6K PS-TFE blend component as a function of normalized sample thicknesses, derived from the fits in Figure 5.

reduction in surface energy from the localization of the low molecular weight fluorocarbon-terminated species. This is in agreement with the previous results of Richards and co-workers.⁶ Indeed, for a given concentration of end-modified material, the surface volume fraction of PS-TFE is consistently around 20% greater than the surface volume fraction of dPS-TFE material. This variation might be explained by the slight difference in molecular weight between the two materials. Lower molecular weights would tend to give a higher surface concentration for the same matrix molecular weight. In our case, however, the lower matrix molecular weight would tend to cancel out this effect. These trends are illustrated more quantitatively by the free energy model developed in the Appendix. Alternatively, the difference in surface coverage could be due to the difference in sample thicknesses, which for the PS-TFE blends averaged 1072 Å compared to 736 Å for the dPS-TFE blends. Thinner films would tend to yield a lower degree of surface coverage, particularly for very thin films, as illustrated by model calculations in the Appendix. For very thin films, surface segregation of the PS-TFE will cause a significant depletion of the end-modified component in the remainder of the film. This is highly unfavorable because of the corresponding reduction in mixing entropy. For increasing film thicknesses, however, the surface-to-volume ratio decreases so that large surface coverages can be achieved without a significant depletion of the concentration in the remainder of the film. (Note that the PS-TFE blend enhancement regions appear consistently shorter due to the film depth normalization procedure.) Similar thickness effects were reported previously for blends of high molecular weight PS and dPS.²¹

In each of the three systems investigated, a slight but notable excess of the low molecular weight component is found at the Si substrate. The substrate enrichment appears to be comparable in each case and also compares well with that observed at the surface of the control blends. While segregation of dPS to silicon oxide has been observed in films of high molecular weight isotopic blends,²¹ the fact that a substrate excess of the low molecular weight component is present even for the 6K PS-TFE/300K dPS system suggests that for our systems, the observed excess can be attributed to molecular weight effects described by Kumar and co-workers.¹⁵

Contact Angle Measurements. Contact angle measurements were conducted on the blend samples used in the NR experiments. The results for the control and end-modified blends are shown in Figure 7a,b, respectively. Contact angles measured from the dPS/PS blends show essentially no dependence on the bulk concentration of 7K dPS material; the average value

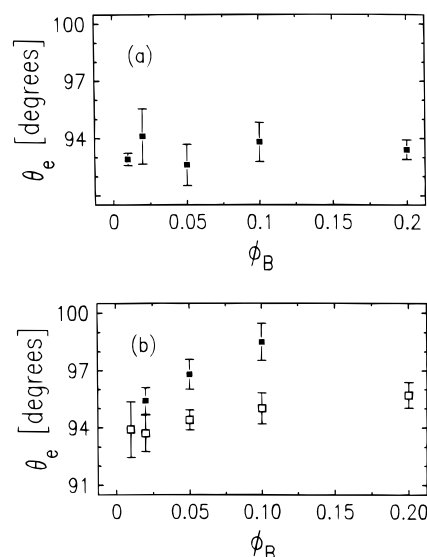


Figure 7. (a) Equilibrium contact angles for the 7K dPS/400K PS blends versus the concentration of dPS. (b) Equilibrium contact angle measurements for the dPS-TFE/PS (□) and PS-TFE/dPS (■) blends versus the concentration of end-modified polymer.

obtained for these blends was 93.4°. This result is qualitatively in agreement with the volume fraction profiles derived from the NR experiments. In the case of the dPS-TFE/PS and PS-TFE/dPS blends, the contact angle is an increasing function of ϕ_B . A comparison between the systems reveals that the magnitude of the contact angles is significantly larger for the PS-TFE blends, again consistent with the NR results.

A more quantitative comparison of the NR and contact angle results can be made by estimating the fractional coverage of the surface by TFE from each technique. From NR, this coverage is calculated from^{23,24}

$$\varphi_{s,\text{TFE}} = \varphi_s \frac{2}{N^{1/2}} \quad (4)$$

where φ_s is the surface fraction of end-modified material. Equation 4 follows from the assumption that the low-energy tails are localized to the surface for all end-modified chains within a coil diameter of the surface.²⁴ From contact angle measurements, $\varphi_{s,\text{TFE}}$ can be determined from¹

$$\cos \theta_e = \varphi_{s,\text{TFE}} \cos \theta_{e,\text{TFE}} + (1 - \varphi_{s,\text{TFE}}) \cos \theta_{e,\text{PS}} \quad (5)$$

where $\theta_{e,\text{PS}}$ is taken as the average value from the control samples. The value of $\theta_{e,\text{TFE}}$ was determined from a PTFE film to be 116°. Figure 8 illustrates the $\varphi_{s,\text{TFE}}$ values obtained from NR (eq 3) and contact angle (eq 4) measurements for the two blend systems. For the PS-TFE/dPS blends, the agreement is quantitative. For the dPS-TFE/PS systems, the same trends with bulk concentration are seen but the NR gives somewhat higher calculated values for the percent surface coverage of TFE.

Conclusions

To summarize the NR results of the A-B/A blend studies, Figure 9 displays the surface concentration of the low molecular weight component versus the bulk concentration for the PS-TFE, dPS-TFE, and control dPS blends. Also shown are theoretical results obtained from free energy models for the two end-modified blend

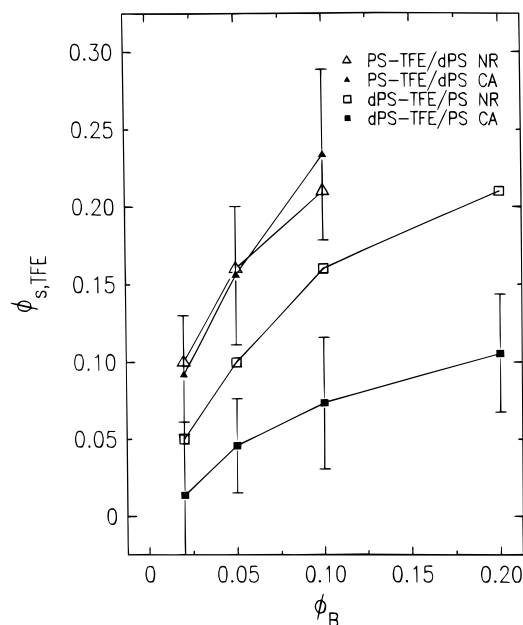


Figure 8. Fluorocarbon surface coverage derived from contact angle and NR results for the PS-TFE/dPS and dPS-TFE/PS blends.

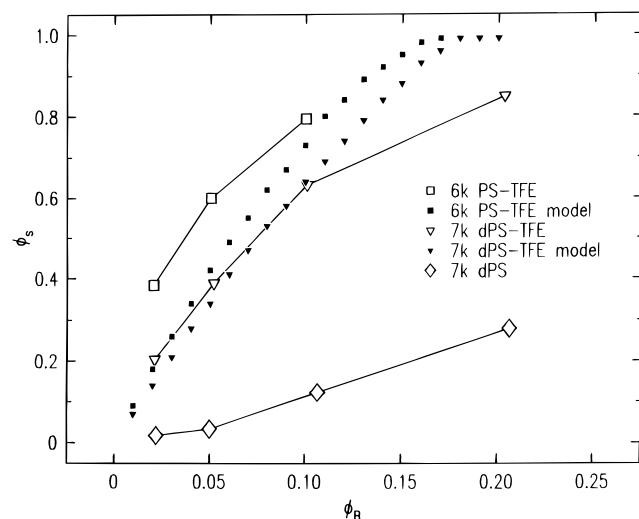


Figure 9. Surface versus bulk concentration of end-modified polymer from NR measurements and free energy model calculations.

systems, detailed in the Appendix. The difference in surface coverage between systems incorporating end-modified materials and those incorporating a low molecular weight PS analog clearly demonstrates that molecular weight effects are small relative to the effect of the low-energy chain ends. This suggests that (1) minimal segregation will be observed at the surface of a polydisperse homopolymer and (2) using molecular weight effects *alone* to produce a surface coverage of functional ends in linear chain systems would not appear feasible. This study further demonstrates that small fractions of low molecular weight end-modified chains blended into commercial plastics can yield significant surface coverages of low-energy chain ends and thereby change the properties of the surface. Since our and other investigations^{5,7} indicate that both chain ends localize to the surface for end-modified chains in the vicinity of the surface, one could expect even more dramatic results using polymers functionalized at both ends. Finally, comparison of the NR results from the

PS-TFE and dPS-TFE blends suggests the importance of film thickness for very thin films. This is supported by the model results, which also show a difference in surface coverage between the two systems deriving primarily from their difference in film thickness.

In general, thermodynamically induced surface segregation of a functionalized polymer component would appear to have significant advantages over other methods of surface modification. Because the surface coverage is dictated by the system thermodynamics, the modified surface should be inherently more robust than surfaces created by kinetic processes where, over time, the surface can reconstruct to lower the free energy. Indeed, the thermodynamic approach to surface modification might be used to prepare "self-healing" surfaces, whereby surface regions which are scratched or worn are regenerated by continued segregation of the functionalized polymer component until its equilibrium surface concentration is reached. Future investigations will focus on the optimization of molecular architecture to gain further control over segregation of functionalized blend components.

Acknowledgment. This work was supported in part by the 3M Innovation Fund and by the National Science Foundation under Grant No. DMR-9357602. The authors wish to acknowledge Dr. Bruce Carvalho for interesting discussions pertaining to this work and Doris Lee for synthesis of the PS-TFE material used in this study.

Appendix: Free Energy Model

Model Description. We have developed a free energy model to make qualitative predictions of the segregation of end-modified polymers to the surface of A-B/A polymer blend thin films. The approach taken is analogous to that used previously to model micelle formation in block copolymer/homopolymer blends.^{25,26} The system consists of a blend film of thickness t with two components, an end-modified polymer (A-B) of N total segments, with short, low-surface energy tails (represented as B), and a homopolymer (A) with N_h segments. Surface localization of the low-energy chain ends is assumed for A-B chains in a near-surface region of depth h . DeGennes has argued that, for surface energy differences between the main chain and the chain ends comparable to the thermal energy, all chains within a distance $2R_G$ from the surface will tend to localize their ends at the surface.²⁴ This assumption is supported by recent studies performed on pure dPS-TFE films.⁷

The overall expression of the free energy which describes this system has the following form:

$$F_{\text{total}} = F_{\text{surf}} + F_{\text{mix}} \quad (\text{A.1})$$

where F_{surf} is the free energy of the near-surface region and F_{mix} is the Flory-Huggins free energy of mixing for the two polymers outside the near-surface region. At the surface, localization of the low-surface energy tails creates a near-surface region composed of anchored chains and interpenetrating homopolymer chains. In the bulk region, end-modified polymers that do not segregate to the surface intermix with unmodified homopolymers.

The free energy F_{surf} of the near-surface region can be broken down into three components as follows:

$$F_{\text{surf}} = A\sigma + F_d + F_m \quad (\text{A.2})$$

where A is the surface area, σ is the surface tension, F_d is the contribution from the deformation of the polymer chains, and F_m is the free energy of mixing for the A-B and A polymers in the near-surface region.

The surface tension has three contributions arising from the A homopolymer, the A segments of surface-localized A-B chains, and their low-energy chain ends:

$$\sigma = \frac{k_b T}{a^2} \left\{ (1 - \varphi_s) \gamma_{A_A} \left(\frac{A - 2pa^2}{A} \right) + \varphi_s \gamma_{A_{AB}} \left(\frac{A - 2pa^2}{A} \right) + \gamma_{B_{AB}} \frac{2pa^2}{A} \right\} \quad (\text{A.3})$$

where φ_s is the fraction of A in the near-surface region contributed by the A-B chains, γ_{A_A} is the reduced surface tension of the A homopolymer, $\gamma_{A_{AB}}$ and $\gamma_{B_{AB}}$ are the reduced surface tensions of the end-modified polymer's A and B components, respectively, p is the number of end-modified chains anchored within the surface area A , a is the segment size (taken as 6.7 Å for PS), and $2pa^2$ is the area of the surface covered with end-modified tails.²³ For $\gamma_{B_{AB}} < \gamma_{A_A}$, this term will be minimized for $p \neq 0$, $\varphi_s \neq 0$, so that segregation will be favored. The dependence of the surface tension on the molecular weight of the blend components is taken into account through the empirical relation:¹

$$\gamma_{A,i} = \gamma_{A,\infty} - k_e N_i^{-2/3} \quad (\text{A.4})$$

From data taken on polystyrene at $T \approx 180^\circ\text{C}$,¹ we obtained the reduced parameters $\gamma_{A,\infty} = 3.32$ and $k_e = 1.87$, while for the fluorocarbon tails at this reference temperature, $\gamma_{B_{AB}}$ was calculated as 0.803.

The deformation energy, F_d , results from a contraction or elongation of the anchored A-B chains from their unperturbed, random coil dimension:²⁷

$$F_d = k_b T p \left[\frac{3}{2} \frac{h^2}{N_A a^2} + \frac{\pi^2}{6} \frac{N_A a^2}{h^2} \right] \quad (\text{A.5})$$

where N_A is the number of statistical segments in the A chain of the end-modified polymer. This term in part counterbalances the first term: While a lower surface energy can be achieved by localizing chain ends, beyond a certain threshold the chains must stretch (as expressed through an increase in h) to accommodate more ends. Eventually, the savings in surface energy are not sufficient to overcome the entropic penalty for unfavorable conformations.

The last contribution to the near-surface free energy, F_m , is the mixing entropy between homopolymer and anchored chains of the end-modified polymer in the near-surface region, given as:

$$F_m = \frac{A h k_b T}{a^3} \left\{ \frac{\varphi_s}{N_A} \ln \varphi_s + \frac{(1 - \varphi_s)}{N_h} \ln(1 - \varphi_s) \right\} \quad (\text{A.6})$$

where N_h is the number of segments per homopolymer chain. The mixing entropy drives the interpenetration of homopolymer in the near-surface region.

Not all end-modified chains in the film will segregate to the near-surface region. The free energy of mixing between the homopolymer and end-modified chains remaining outside the near-surface region, F_{mix} , is given by:²⁵

$$F_{\text{mix}} = k_b T \Omega (1 - \varphi_B \nu \Lambda) \left\{ \frac{\varphi_1}{N} \ln \varphi_1 + \frac{(1 - \varphi_1)}{N_h} \ln(1 - \varphi_1) \right\} \quad (\text{A.7})$$

where Ω is the total number of monomers in the system, φ_B is the initial bulk concentration of A-B, ν is the fraction of end-modified polymer which segregates to the near-surface region, $\varphi_B \nu \Lambda$ is the volume fraction of the system occupied by the near-surface region, with Λ , the ratio of the volume of the near-surface region to the near-surface volume occupied by A-B chains, defined as

$$\Lambda = 1 - \frac{N_A}{N} \left(1 - \frac{1}{\varphi_s} \right) \quad (\text{A.8})$$

and φ_1 is the concentration of end-modified polymer remaining in the bulk region at equilibrium

$$\varphi_1 = \frac{\varphi_B (1 - \nu)}{(1 - \varphi_B \nu \Lambda)} \quad (\text{A.9})$$

Equation A.7 neglects the energetic interaction between the A and B components in the bulk. For certain systems, however, this is known to be significant²⁸ and should be incorporated into the bulk free energy of mixing. In general, this term tends to counter segregation of the A-B chains to the surface.

Constant density of the system is imposed through the incompressibility condition:

$$\Omega a^3 = A t \quad (\text{A.10})$$

In the near-surface region, the number of segments contributed by the end-modified polymer chains, pN , is related to Ω through:

$$pN = \Omega \varphi_B \nu \quad (\text{A.11})$$

Additionally, h can be eliminated from the model equations by redefining it in terms of the system's other parameters:

$$h = p N \Lambda \frac{a^3}{A} \quad (\text{A.12})$$

Using eqs A.10–A.12, the free energy is recast in terms of two variables: φ_s and ν . To obtain solutions, the total free energy of the system per monomer, $F_{\text{total}}/k_b T \Omega$, is minimized with respect to these two variables for a given set of parameters φ_B , N , N_h , and t .

Model Results. Three sets of parameter variations were performed to predict the degree of segregation in PS-TFE/PS blend films. In the first set of model variations, the fraction of PS-TFE in the near-surface region (φ_s) was studied as a function of the bulk concentration (φ_B) for three different matrix molecular weights. The number of segments in the end-modified additive was held constant in this series at $N = 65$, modeling a 7K dPS-TFE material. The matrix molecular weights were chosen as $N_h = 39$, 386, and 3856, modeling a 4K, 40K, and 400K PS matrix, respectively. The sample thickness, t , was held constant at 750 Å. The results of the matrix molecular weight variations can be seen in Figure 10. With increasing matrix molecular weight, the fraction of end-modified material near the surface increases for any given value of φ_B . As the matrix molecular weight increases, the entropy of mixing decreases (eqs A.6 and A.7), while the energetic

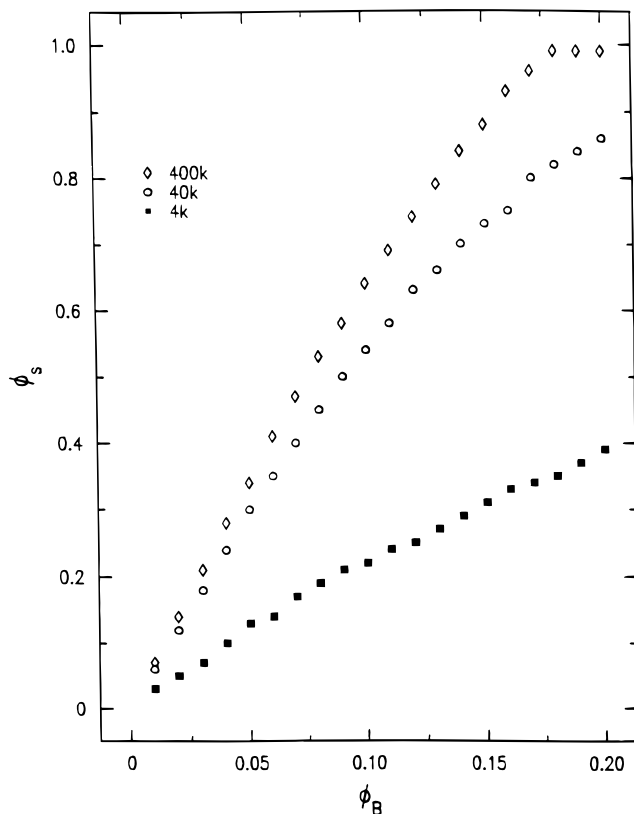


Figure 10. Model results of surface versus bulk concentration of 7K dPS-TFE in PS for three matrix molecular weights, with $t = 750 \text{ \AA}$.

savings afforded by localizing the low-energy chain ends near the surface increase (eq A.3). The degree of segregation additionally increases with increasing bulk concentration of dPS-TFE. For the 400K matrix blends, φ_s reaches 100% for a bulk concentration of 17.5%.

In applications where mechanical properties of the interface are important, longer anchoring chains may be desirable to improve the interpenetration of the homopolymer with the segregated chains. Thus in the second set of model variations, φ_s is studied as a function of φ_B for three different additive molecular weights while the matrix was held constant at $N_h = 2679$, modeling a 300K PS homopolymer. The additive sizes were $N = 58, 97$, and 290 , corresponding to a 6K, 10K, and 30K dPS-TFE material, respectively. The sample thickness was held constant at 1200 \AA . The results of the additive molecular weight variations can be seen in Figure 11. The trend of increasing φ_s with decreasing N can be seen for any given value of φ_B . Still, significant coverages are predicted for higher molecular weight additives. However, since the number of chain ends per unit surface area also decreases with increasing N , so the ability to modify surface properties is limited.

The last model variation carried out was a test of the degree of segregation as a function of the sample's thickness, t , keeping the molecular weights constant at $N = 65$ (7K) and $N_h = 386$ (40K) and φ_B fixed at 0.05 . The results are shown in Figure 12 for the thickness range $200 \text{ \AA} < t < 1 \text{ \mu m}$. The overall trend is for increasing φ_s as the sample thickness increases. For very thin films, any appreciable amount of additive segregation would significantly deplete the concentration in the remainder of the film; this is unfavorable from the standpoint of mixing entropy. For thicker samples the surface-to-volume ratio decreases and an

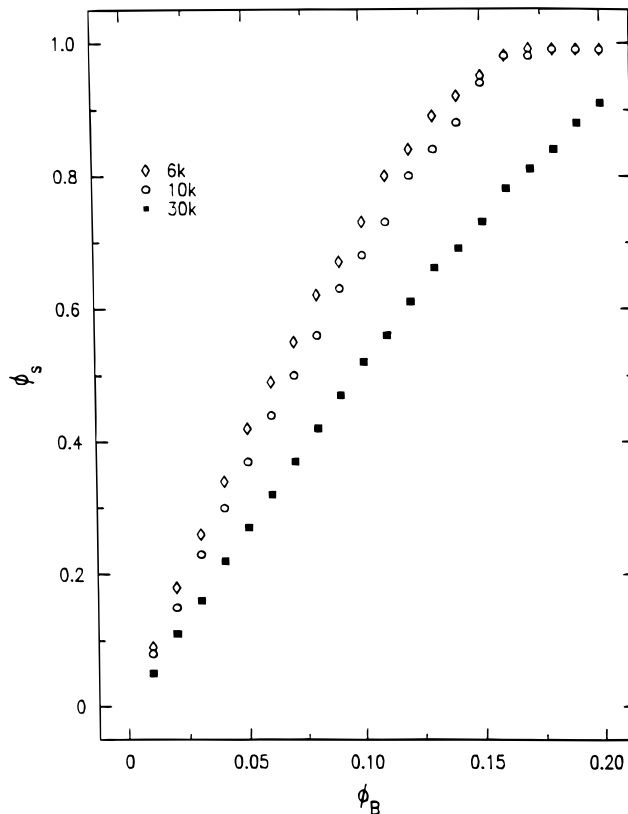


Figure 11. Model results of surface versus bulk concentration of PS-TFE in 300K dPS for three additive molecular weights, with $t = 1200 \text{ \AA}$.

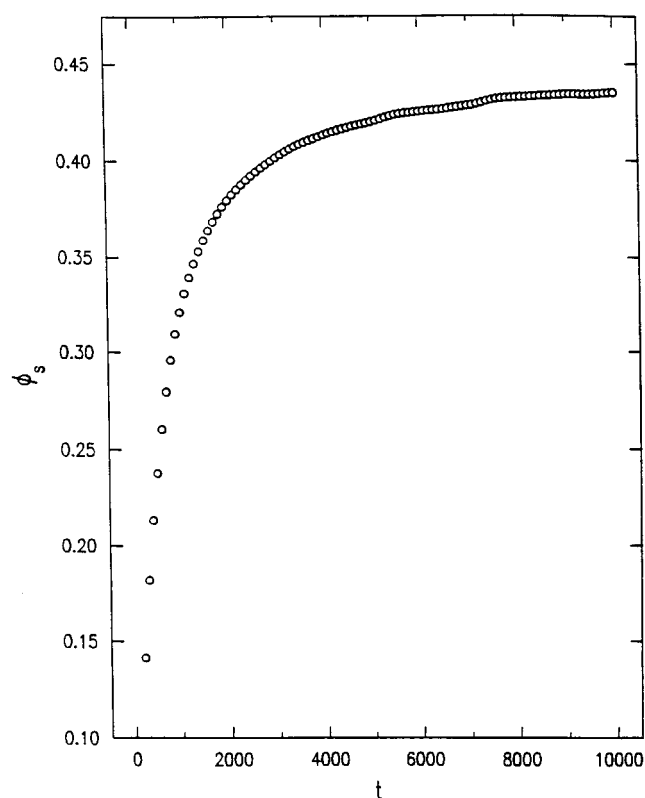


Figure 12. Model results of surface concentration versus film thickness for a 5% blend of 7K dPS-TFE in 400K PS.

increase in the surface concentration is energetically favorable. The surface fraction of end-modified chains saturates with increasing thickness, asymptotically approaching 0.45.

While our model considers segregation only to the air surface of the film, experimentally a slight excess of the low molecular weight component was always observed at the substrate. In very thin films, this substrate adsorption would be expected to compete with surface segregation, resulting in a more pronounced thickness effect.

References and Notes

- (1) Wu, S. *Polymer Interface and Adhesion*; Marcel Dekker: New York, 1982.
- (2) Garbassi, F.; Morra, M.; Occhiello, E. *Polymer Surfaces: From Physics to Technology*; John Wiley and Sons: New York, 1994.
- (3) Hunt, M. O.; Belu, A.; Linton, R.; DeSimone, J. M. *Macromolecules* **1993**, *26*, 4854.
- (4) Jalbert, C. J. Ph.D. Thesis, University of Connecticut, 1993.
- (5) Elman, J. F.; Johs, B. D.; Long, T. E.; Koberstein, J. T. *Macromolecules* **1994**, *27*, 5341.
- (6) Affrossman, S.; Hartshorne, M.; Kiff, T.; Pethrick, R. A.; Richards, R. W. *Macromolecules* **1994**, *27*, 1588.
- (7) Schaub, T. F. SM Thesis, Massachusetts Institute of Technology, Cambridge, MA, 1995.
- (8) Jalbert, C.; Koberstein, J. T.; Yilgor, I.; Gallagher, P.; Krukoni, V. *Macromolecules* **1993**, *26*, 3069.
- (9) Jalbert, C. J.; Koberstein, J. T.; Balaji, R.; Bhatia, Q.; Salvati, L.; Yilgor, I. *Macromolecules* **1994**, *27*, 2409.
- (10) Fleischer, C. A.; Morales, A. R.; Koberstein, J. T. *Macromolecules* **1994**, *27*, 379.
- (11) Norton, L. J.; Smigolova, V.; Pralle, M. U.; Hubenko, A.; Dai, K. H.; Kramer, E. J.; Hahn, S.; Berglund, C.; DeKoven, B. *Macromolecules* **1995**, *28*, 1999.
- (12) Scott, C. E.; Macosko, C. W. *Polymer* **1994**, *35*, 5422.
- (13) Scott, C.; Macosko, C. *J. Polym. Sci., Part B: Polym. Phys.* **1994**, *32*, 205.
- (14) Chen, X.; Gardella, J. A. *Macromolecules* **1994**, *27*, 3363.
- (15) Hariharan, A.; Kumar, S. K.; Russell, T. P. *Macromolecules* **1990**, *23*, 3584.
- (16) Kaiser, H.; Hamacher, K.; Kulasekere, R.; Lee, W.-T.; Ankner, J. F.; DeFacio, B.; Miceli, P.; Worcester, D. L. *Proc. SPIE-Int. Soc. Opt. Eng.* **1994**, *2241*, 78.
- (17) Russell, T. P. *Mater. Sci. Rep.* **1990**, *5*, 171.
- (18) Mayes, A. M.; Russell, T. P.; Satija, S. K.; Majkrzak, C. F. *Macromolecules* **1992**, *25*, 5677.
- (19) Parratt, L. G. *J. Chem. Phys.* **1956**, *53*, 597.
- (20) Jones, R. A. L.; Kramer, E. J.; Rafailovich, M. H.; Sokolov, J.; Schwartz, S. A. *Phys. Rev. Lett.* **1989**, *62*, 280.
- (21) Hariharan, A.; Kumar, S. K.; Rafailovich, M. H.; Sokolov, J.; Zheng, X.; Duong, D.; Schwarz, S. A.; Russell, T. P. *J. Chem. Phys.* **1993**, *99*, 656.
- (22) Hong, P. P.; Boerio, F. J.; Smith, S. D. *Macromolecules* **1994**, *27*, 596.
- (23) The areal contribution of the TFE tails is estimated here as ca. 2 times the segmental area of PS.
- (24) DeGennes, P.-G. R. *Acad. Sci. (Paris)* **1988**, *307*, 1841.
- (25) Leibler, L.; Orland, H.; Wheeler, J. C. *J. Chem. Phys.* **1983**, *79*, 3550.
- (26) Mayes, A. M.; Olvera de la Cruz, M. *Macromolecules* **1988**, *21*, 2543.
- (27) Carslaw, H. S.; Jaeger, J. C. *Conduction of Heat in Solids*, 2nd ed.; Oxford University Press: London, 1959; pp 198–99, 233, 331, 335–336, 366–370.
- (28) Fleischer, C. A.; Koberstein, J. T.; Krukoni, V.; Wetmore, P. A. *Macromolecules* **1993**, *26*, 4172.

MA9510810